Block-Differential Modulation Over Doubly Selective Wireless Fading Channels

Alfonso Cano, *Student Member, IEEE*, Xiaoli Ma, *Member, IEEE*, and Georgios B. Giannakis, *Fellow, IEEE*

***Abstract*—Differential encoding is known to simplify receiver implementation because it by-passes channel estimation. However, over rapidly fading wireless channels, extra transceiver modules are necessary to enable differential transmission. Relying on a basis expansion model for time and frequency selective (doubly selective) channels, we derive such a generalized block-differential (BD) codec and prove that it achieves maximum Doppler and multipath diversity gains, while affording low-complexity maximum-likelihood decoding. We further show that existing BD systems over frequency-selective or time-selective channels follow as special cases of our novel system. Simulations using the widely accepted Jakes' model corroborate our theoretical analysis.**

***Index Terms*—Differential encoding, diversity, Doppler, doubly selective channels, multipath.**

I. Introduction

HIGH data-rate mobile links are characterized by frequency selectivity due to multipath propagation, as well as time selectivity arising from relative transmitter–receiver motion, oscillator drifts, or phase noise. When considered together, these two effects constitute what we term doubly selective fading, which critically affects error performance over rapidly fading wireless channels. Fading has been traditionally mitigated using diversity techniques [17]. Frequency-selective channels offer multipath diversity, whereas time-selective channels provide Doppler diversity. In doubly selective channels, the diversity can be as high as the product of the two (multipath times Doppler) [2], [14], [18].

When channel state information (CSI) is not available at the receiver, pilot-symbol aided modulation (PSAM) has been derived for doubly selective links to obtain minimum mean-square error (MMSE) channel estimates, while at the same time maximizing a lower bound on the ergodic capacity [16]. The PSAM pattern of [16] leads to a two-dimensional channel estimator at the receiver, but the rich diversity provided by the channel may not be guaranteed.

Differential schemes can obviate channel estimation and, if designed properly, they are capable of achieving the available diversity at the price of signal-to-noise ratio (SNR) loss, as well as decoding delay. The merits of differential phase-shift keying (DPSK) have been well documented over time-invariant links [17]. However, conventional differential detectors (DD) exhibit error floor if the channel varies from symbol to symbol [20]. Challenged by this fact, differential designs over time-varying (TV) links have been pursued recently. Existing approaches use multiple-symbol detection (MSD) [6] or decision-feedback differential detection (DF-DD) (see [20] and references therein), but do not exploit Doppler diversity while they entail relatively high complexity. Designs aiming at Doppler diversity date back to [3], which relied on repetition coding. Recently, two more encoding schemes have exploited Doppler diversity: the differential modulation diversity (DMD) technique in [19], and the block-differential (BD) scheme in [15]. The first one combines interleaving with DF-DD. The second scheme is based on the basis expansion model (BEM) of [4] and comes in two flavors: BD design I relies on time-frequency duality, and BD design II uses DF-DD.

Differential designs have also been developed to collect other types of diversity. Differential unitary space–time modulation (DUSTM) can benefit from spatial diversity that becomes available with multiple antennas, but has been introduced only for flat-fading channels [7], [8]. For frequency-selective channels, one can certainly rely on orthogonal frequency-division multiplexing (OFDM) and differentially encode across flat-fading subcarriers, through which maximum multipath diversity can be effected through channel coding [1], or by a proper carrier grouping employing DUSTM across each group [12]. However, when the channel is TV, error performance of differential OFDM degrades. Developing differential schemes when *both* time and frequency selectivity are present remains largely an uncharted territory.

In this paper, we derive a novel BD system over doubly selective channels. We model each block of symbols using the BEM. Based on (de-) interleaving, (inverse) fast Fourier transform ((I)FFT) operations along with insertion and removal of cyclic prefix (CP) segments and a block repetition encoder, we exploit the circularity of the channel via a repeated OFDM-like encoding per subblock (Section III). Our receiver collects

Paper approved by X. Dong, the Editor for Modulation and Signal Design of the IEEE Communications Society. Manuscript received September 23, 2004; revised April 18, 2005. Work in this paper was prepared through collaborative participation in the Communications and Networks Consortium sponsored by the U.S. Army Research Laboratory under the Collaborative Technology Alliance Program, Cooperative Agreement DAAD19-01-2-0011. The U.S. Government is authorized to reproduce and distribute reprints for Government purposes notwithstanding any copyright notation thereon. The work of the second author was supported by the Army Research Office under Grant W911NF-04-1-0338. The work of the third author was supported in part by the Italian Minister of University and Research under PRIN 2002 Project "MC-CDMA: An air interface for the 4th generation of wireless systems." This paper was presented in part at the International Conference on Communications, Seoul, Korea, May 2005.

A. Cano is with the Area of Signal Theory and Communications, Rey Juan Carlos University, 28943 Fuenlabrada (Madrid), Spain (e-mail: alfonso.cano@urjc.es).

X. Ma is with the Department of Electrical and Computer Engineering, Auburn University, Auburn, AL 36849 USA (e-mail: xiaoli@auburn.edu).

G. B. Giannakis is with the Department of Electrical and Computer Engineering, University of Minnesota, Minneapolis, MN 55455 USA (e-mail: georgios@ece.umn.edu).

Digital Object Identifier 10.1109/TCOMM.2005.860038

full multipath-Doppler diversity gain (derived in Section VI), can afford reduced maximum-likelihood (ML) complexity (Section IV), and provides bandwidth efficiency comparable to any BD-OFDM system (Section V). The price paid for these nice features is coding-gain loss, which increases with the degree of channel variation, as we quantify in the performance analysis of Section VI. Finally, simulations in Section VII verify our analytical claims, and Section VIII concludes the paper.

Notation: Upper (lower) bold face letters are used for matrices (column vectors); $(\cdot)^{\mathcal{H}}$ and $(\cdot)^T$ denote Hermitian and transpose; $\lceil\cdot\rceil$ and $\lfloor\cdot\rfloor$ are integer ceiling and floor; $[\cdot]_{k,l}$ denotes the (k,l)th entry of a matrix, and $[\cdot]_k$ the kth entry of a vector; $\mathbf{I}_N$ denotes the $N\times N$ identity matrix; $\mathbf{1}_N$ is the $N\times 1$ all-one vector; $\mathbf{0}_{N\times M}$ denotes the $N\times M$ all-zero matrix and $\mathbf{0}_N$ is the $N\times 1$ all-zero vector; $\otimes$ denotes Kroneker product; $\mathrm{diag}(\mathbf{x})$ is a diagonal matrix with $\mathbf{x}$ on its diagonal; $\det(\mathbf{X})$ is the determinant of matrix $\mathbf{X}$; $\mathrm{mod}[m,n]$ is the remainder after dividing m by n; and $\mathbf{F}_N$ stands for the normalized FFT matrix with entries $[\mathbf{F}_N]_{k,l}:=N^{-1/2}\exp(-j2\pi kl/N)$.

II. System Model

Let $h(t;\tau)$ be the continuous-time impulse response of a general doubly selective fading channel which includes transmit and receive filters, as well as channel propagation effects. The multipath spread $\tau_{\max}$ bounds the delays τ caused by multipath, while the Doppler spread $f_{\max}$ bounds the time variations induced by Doppler effects. We will take the sampling period at the receiver equal to the symbol period T_s. Consider now a block of N symbols $\{x_k(n)\}_{n=0}^{N-1}$, where $k:=\lfloor n/N\rfloor$ denotes block index. Because the channel is approximately bandlimited, during each block of time $t\in[kNT_s,(k+1)NT_s)$, the channel variation of each path (say, the lth) can be represented by $(Q+1)$ coefficients $\{h_q(k;l)\}_{q=0}^{Q}$ that remain invariant per block, but are allowed to change with k. Time variation in $h(t;\tau)$ is captured by a finite set of Fourier bases. Under these conditions, our *baseband-sampled-equivalent* channel model can be written as

$$h^{(k)}(n;l)=\sum_{q=0}^{Q}h_q(k;l)e^{j\omega_q n},\quad l\in[0,L] \tag{1}$$

where $\omega_q:=2\pi(q-Q/2)/N$, $L:=\lceil\tau_{\max}/T_s\rceil$ and $Q:=2\lceil f_{\max}NT_s\rceil$. Equation (1) is the BEM introduced for doubly selective channels in [4]. The bounds $\tau_{\max}$ and $f_{\max}$ can be experimentally measured (e.g., via sounding techniques), so, we will henceforth adopt the following.

Assumption 1: Parameters $\tau_{\max}$ and $f_{\max}$ are bounded, known, and satisfy $2f_{\max}\tau_{\max}<1$.

The reason for requiring $2f_{\max}\tau_{\max}<1$ will become clear in Section V, and is satisfied by mobile wireless channels that are typically underspread [17, p. 816]. We can factor $h^{(k)}(n;l)$ in (1) as

$$h^{(k)}(n;l)=\mathbf{w}_n^T\mathbf{h}(k;l)\quad\forall n\in[0,N-1],l\in[0,L] \tag{2}$$

with $\mathbf{w}_n:=[e^{j\omega_0 n},\ldots,e^{j\omega_Q n}]^T$ capturing time variation, and $\mathbf{h}(k;l):=[h_0(k;l),\ldots,h_Q(k;l)]^T$ collecting the channel's time-invariant coefficients. We have $(L+1)$ vectors $\{\mathbf{h}(k;l)\}_{l=0}^{L}$ of $(Q+1)$ coefficients each, for a total of $(Q+1)(L+1)$ coefficients. For performance-analysis purposes, we will further need the following.

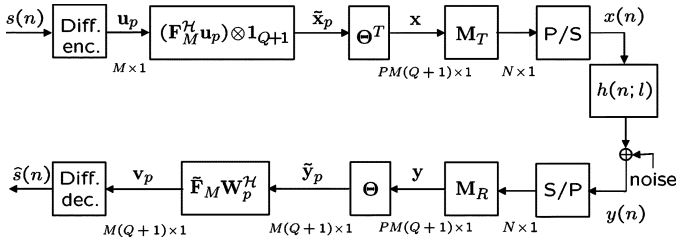

Fig. 1. Baseband-sampled-equivalent system model.

Assumption 2: The $(Q+1)(L+1)$ BEM coefficients $h_q(k;l)$ are zero-mean, complex Gaussian random variables and remain invariant over each block k of N symbols. A new set of BEM coefficients is considered every NT_s seconds.

Note that the row vector $\mathbf{w}_n^T$ in (2) does not depend on k. With the Fourier bases available, the $(L+1)(Q+1)$ BEM coefficients $h_q(k;l)$ are thus the only *unknowns* characterizing the doubly selective channel inside each (here, the kth) block of N symbol periods.

With reference to Fig. 1, the nth sample in the kth received block, $y_k(n)$, is the noisy output of the doubly selective channel $h^{(k)}(n;l)$ in (1), with input the transmitted symbol $x_k(n)$

$$y_k(n)=\sum_{l=0}^{L}h^{(k)}(n;l)x_k(n-l)+z_k(n) \tag{3}$$

where $z_k(n)$ is additive white Gaussian noise (AWGN) with zero mean and variance $N_0/2$.

Our main goal is to design $x_k(n)$ properly, so that based on $y_k(n)$ in (3), decoding can be accomplished without estimating the $(Q+1)(L+1)$ coefficients $h_q(k;l)$. Because we will be working inside the kth block, for notational simplicity, we will drop index k in our subsequent derivations.

III. Block-Differential (BD) Design

In this section, we will introduce our BD encoder and decoder. The baseband-sampled-equivalent system model is depicted in Fig. 1. We will start from the outer to the inner encoders at the transmitter side, and proceed through the channel to the inner and outer decoders at the receiver.

A. BD Encoding, Cyclic Prefixing, and (De) Interleaving

Fig. 2 depicts the structure of our differential encoder. Information symbols $\{s(n)\}$ drawn from a finite alphabet $\mathcal{A}_s$ are parsed into blocks $\mathbf{s}_p$ of size $M(Q+1)$, indexed by p and mapped one-to-one to an $M\times M$ diagonal generator matrix $\mathbf{D}_{g_p}$. The latter is used to yield differentially encoded blocks $\mathbf{u}_p$ according to the recursion

$$\mathbf{u}_p=\begin{cases}\mathbf{D}_{g_p}\mathbf{u}_{p-1}, & p\geq 1\\ \mathbf{1}_M, & p=0.\end{cases} \tag{4}$$

The M diagonal entries of $\mathbf{D}_{g_p}$ are drawn from a finite alphabet $\mathcal{A}_g$. Let R be the transmission rate defined as the number of bits transmitted per channel use. In order to support rate R, we need to properly map information symbols to the corresponding transmitted symbols. Since the diagonal of $\mathbf{D}_{g_p}$ has size M, we need the cardinalities of the alphabets to satisfy

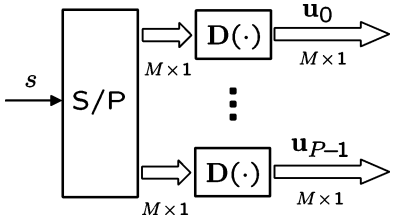

Fig. 2. BD encoder in (4).

$|\mathcal{A}_g|^M = |\mathcal{A}_s|^{M(Q+1)}$. Comparing $\mathcal{A}_s$ with $\mathcal{A}_g$, we recognize that our BD encoder increases the constellation size. Intuitively, we expect this increase to degrade error performance.

Subsequently, we take the IFFT of $\mathbf{u}_p$ and repeat $Q+1$ times the resultant subblock of size M, as described through the Kronecker product operation (see also Fig. 1)

$$\tilde{\mathbf{x}}_p := \left(\mathbf{F}_M^{\mathcal{H}}\mathbf{u}_p\right) \otimes \mathbf{1}_{Q+1}. \tag{5}$$

The encoding in (5) has similarities with the one used by [10] in the context of OFDM to reduce peak-to-average-power ratio. In our pursuit of BD encoding for doubly selective channels, (5) will play an instrumental role in: 1) isolating and annihilating the TV part from the time-invariant coefficients of the BEM (through the repetitive part); and 2) diagonalizing (similar to OFDM) the resultant circulant matrix of the time-invariant channel factor of the BEM (via $\mathbf{F}_M^{\mathcal{H}}$ and CP insertion; and a mirror CP removal and FFT operation at the receiver).

Our next step is interleaving, which is critical for enabling the diversity gains of our BD encoder. Interleaving is implemented by the following $PM(Q+1)\times PM(Q+1)$ permutation matrix:

$$\mathbf{\Theta} := \begin{bmatrix} \mathbf{I}_{(Q+1)} \otimes \mathbf{e}_1^T \\ \vdots \\ \mathbf{I}_{(Q+1)} \otimes \mathbf{e}_{PM}^T \end{bmatrix} \tag{6}$$

where $\mathbf{e}_m^T$ is the mth row of matrix $\mathbf{I}_{PM}$, $\forall m \in [1, PM]$. With $\tilde{\mathbf{x}}_p$ as in (5) and $\tilde{\mathbf{x}} := [\tilde{\mathbf{x}}_0^T, \ldots, \tilde{\mathbf{x}}_{P-1}^T]^T$, the interleaver output is $\mathbf{x} := \mathbf{\Theta}^T\tilde{\mathbf{x}}$.

When transmitted through the channel, each block $\mathbf{x}$ and its subblocks are affected by interblock interference (IBI) caused by the channel delay spread of order L, which can be avoided using a CP of length L. For reasons that will become clear later, we partition $\mathbf{x}$ into $P(Q+1)$ subblocks, each consisting of M symbols, and insert in every subblock a CP segment of size L. Concatenating these CP-augmented subblocks, we create a block $\bar{\mathbf{x}}$ of size $N = P(M+L)(Q+1)$. As with OFDM, CP insertion costs bandwidth and power, but in our case, it also facilitates processing of the IBI-free subblocks. Insertion and removal of CP segments from each subblock of $\mathbf{x}$ can be described, respectively, with the matrices

$$\mathbf{M}_T := \mathbf{I}_{P(Q+1)} \otimes \mathbf{T}_{\mathrm{CP}}, \quad \mathbf{M}_R := \mathbf{I}_{P(Q+1)} \otimes \mathbf{R}_{\mathrm{CP}} \tag{7}$$

where $\mathbf{T}_{\mathrm{CP}}$ ($\mathbf{R}_{\mathrm{CP}}$) is an $(M+L)\times M$ (respectively, $M\times(M+L)$) matrix implementing insertion (removal) of CP per subblock of size M. As in [14], we define them as $\mathbf{T}_{\mathrm{CP}} := [\mathbf{I}_N^{(L)}, \mathbf{I}_M]^T$ and $\mathbf{R}_{\mathrm{CP}} := [\mathbf{0}_{M\times L}, \mathbf{I}_M]$, where $\mathbf{I}_N^{(L)}$ denotes the last L columns of $\mathbf{I}_N$.

With CP segments inserted, $\mathbf{x}$ is augmented to the $N\times 1$ block $\bar{\mathbf{x}} := \mathbf{M}_T\mathbf{x}$. After parallel-to-serial (P/S) conversion, $\bar{\mathbf{x}}$ is transmitted through the channel in (2). Let the received $N\times 1$ block after serial-to-parallel (S/P) conversion be denoted as $\bar{\mathbf{y}}$. Upon removing the CP segments at the receiver, we obtain $\mathbf{y} := \mathbf{M}_R\bar{\mathbf{y}}$, obeying the matrix-vector input/output (I/O) relationship

$$\mathbf{y} = \mathbf{H}\mathbf{x} + \mathbf{z} \tag{8}$$

where $\mathbf{H}$ denotes the $PM(Q+1)\times PM(Q+1)$ block diagonal channel matrix. Because CP insertion and removal operations eliminate IBI, $\mathbf{H}$ is given by

$$\mathbf{H} := \begin{bmatrix} \mathbf{H}_0 & \mathbf{0} & \ldots & \mathbf{0} \\ \mathbf{0} & \mathbf{H}_1 & & \\ \vdots & & \ddots & \vdots \\ \mathbf{0} & \ldots & \mathbf{0} & \mathbf{H}_{P(Q+1)-1} \end{bmatrix} \tag{9}$$

and upon defining $M_i := iM + (i+1)L$ for brevity, the ith $M\times M$ matrix entry $\mathbf{H}_i$ is shown in (10).

If time-selectivity were absent, $h(M_i+m;l)$ would not depend on i or m, and $\mathbf{H}_i$ would have been a square circulant matrix. Such circulant matrices of frequency-selective channels can clearly be diagonalized using FFT and IFFT operations, as shown in (10) at the bottom of the page.

We next deinterleave $\mathbf{y}$ to obtain $\tilde{\mathbf{y}} := \mathbf{\Theta}\mathbf{y}$, and rewrite the I/O relationship (8) as

$$\tilde{\mathbf{y}} = \tilde{\mathbf{H}}\tilde{\mathbf{x}} + \tilde{\mathbf{z}} \tag{11}$$

with $\tilde{\mathbf{H}} := \mathbf{\Theta}\mathbf{H}\mathbf{\Theta}^T$. Since $\mathbf{\Theta}^T\mathbf{\Theta} = \mathbf{I}_{PM(Q+1)}$, $\tilde{\mathbf{z}}$ is still AWGN with the same variance. Notice that $\tilde{\mathbf{H}}$ in (11) is also a block-diagonal matrix

$$\tilde{\mathbf{H}} := \begin{bmatrix} \tilde{\mathbf{H}}_0 & \mathbf{0} & \ldots & \mathbf{0} \\ \mathbf{0} & \tilde{\mathbf{H}}_1 & & \vdots \\ \vdots & & \ddots & \vdots \\ \mathbf{0} & \ldots & \mathbf{0} & \tilde{\mathbf{H}}_{P-1} \end{bmatrix} \tag{12}$$

where, in accordance with $\mathbf{H}_i$, its pth $M(Q+1)\times M(Q+1)$ submatrix in (13) exhibits circularity in l; and upon defining

$$\mathbf{H}_i := \begin{bmatrix} h(M_i;0) & 0 & \ldots & h(M_i;L) & \ldots & h(M_i;1) \\ h(M_i+1;1) & h(M_i+1;0) & \ddots & 0 & h(M_i+1;L) & \vdots \\ \vdots & \vdots & \ddots & & \ddots & \ddots \\ h(M_i+L;L) & \ldots & \ldots & h(M_i+L;0) & \ldots & 0 \\ \vdots & \ddots & & \ddots & & \vdots \\ 0 & \ldots & 0 & h(M_i+M-1;L) & \ldots & h(M_i+M-1;0) \end{bmatrix} \tag{10}$$

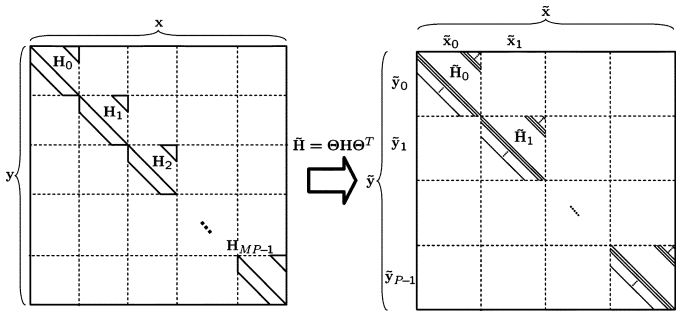

Fig. 3. Structure of matrices $\mathbf{H}$ and $\bar{\mathbf{H}}$ in (9) and (12), respectively.

$M_{p,q} := (p + q(Q+1))M + (p + q(Q+1) + 1)L$, each $(Q+1) \times (Q+1)$ matrix $\tilde{\mathbf{H}}_{p,m}(l)$ in (13) can be written as shown in (13) at the bottom of the page

$$\tilde{\mathbf{H}}_{p,m}(l) := \mathrm{diag}\left(h(M_{p,0}+m;l), h(M_{p,1}+m;l), \ldots, h(M_{p,Q}+m;l)\right) \quad (14)$$

$\forall p \in [0, P-1]$, $q \in [0, Q]$, and $l \in [0, L]$. Fig. 3 depicts the structure of $\mathbf{H}$ and $\tilde{\mathbf{H}}$. Coming back to (11), and partitioning $\tilde{\mathbf{y}}$ into P subblocks of size $M(Q+1)$ each, we can express the matrix-vector I/O relationship on a per-subblock basis as

$$\tilde{\mathbf{y}}_p = \tilde{\mathbf{H}}_p \tilde{\mathbf{x}}_p + \tilde{\mathbf{z}}_p, \quad p \in [0, P-1] \quad (15)$$

where $[\tilde{\mathbf{y}}_p]_k := [\tilde{\mathbf{y}}]_{pM(Q+1)+k}$ $\forall k \in [1, M(Q+1)]$, and $\tilde{\mathbf{x}}_p$ is given in (5).

B. Subblock Invariant and Diagonal I/O Relationship

Recall that the subblocks $\tilde{\mathbf{x}}_p$ in (15) contain $Q+1$ repetitions of the IFFT-processed subblocks $\mathbf{u}_p$ [c.f. (5)], which are differentially encoded through the diagonal generator matrix $\mathbf{D}_{g_p}$ [c.f. (4)]. Exploiting this structure of $\tilde{\mathbf{x}}_p$, our objective in this subsection is to show that (15) can be reduced to an I/O relationship, where $\tilde{\mathbf{H}}_p$ is replaced by a channel matrix that is diagonal and not a function of p. This diagonal and time-invariant (with respect to (w.r.t.) p) I/O relationship will allow us to differentially decode $\mathbf{u}_p$ from the received subblocks $\tilde{\mathbf{y}}_p$. To this end, our first task is to isolate the invariant part of $\tilde{\mathbf{H}}_p$, a step we summarize next (see Appendix A for the proof).

Proposition 1: If the input $\tilde{\mathbf{x}}_p$ in (15) has the repetitive structure (5), then (15) reduces to the I/O $\tilde{\mathbf{y}}_p = (Q+1)^{-1} \mathbf{W}_p \mathbf{H}_c \tilde{\mathbf{x}}_p + \tilde{\mathbf{z}}_p$, where $\tilde{\mathbf{H}}_p$ has been factored in two square matrices: one captures the TV Fourier bases

$$\mathbf{W}_p := \begin{bmatrix} \mathbf{W}_{p,0} & \mathbf{0} & \ldots & \mathbf{0} \\ \mathbf{0} & \mathbf{W}_{p,1} & & \\ \vdots & & \ddots & \vdots \\ \mathbf{0} & \ldots & \mathbf{0} & \mathbf{W}_{p,M-1} \end{bmatrix} \quad (16)$$

and the other factor remains invariant across the subblocks $\{\tilde{\mathbf{x}}_p\}_{p=0}^{P-1}$

$$\mathbf{H}_c := \begin{bmatrix} \mathbf{H}_c(0) & \mathbf{0} & \ldots & \mathbf{H}_c(L) & \ldots & \mathbf{H}_c(1) \\ \mathbf{H}_c(1) & \mathbf{H}_c(0) & \ddots & \mathbf{0} & \mathbf{H}_c(L) & \vdots \\ \vdots & \vdots & \ddots & & \ddots & \ddots \\ \mathbf{H}_c(L) & \mathbf{H}_c(L-1) & \ldots & \mathbf{H}_c(0) & \ldots & \mathbf{0} \\ \vdots & \ddots & & & \ddots & \vdots \\ \mathbf{0} & \ldots & \mathbf{0} & \mathbf{H}_c(L) & \ldots & \mathbf{H}_c(0) \end{bmatrix} \quad (17)$$

where each $(Q+1) \times (Q+1)$ submatrix $\mathbf{W}_{p,m}$ in (16) is $\mathbf{W}_{p,m} := [\mathbf{w}_{M_{p,0}+m}, \ldots, \mathbf{w}_{M_{p,Q}+m}]^T$, and each $(Q+1) \times (Q+1)$ submatrix in (17) is $\mathbf{H}_c(l) := \mathbf{1}_{Q+1}^T \otimes \mathbf{h}(l)$. □

We stress that the factorization $\tilde{\mathbf{H}}_p = (Q+1)^{-1} \mathbf{W}_p \mathbf{H}_c$ holds only when $\tilde{\mathbf{x}}_p$ has the repetitive structure $\tilde{\mathbf{x}}_p = (\mathbf{F}_M^{\mathcal{H}} \mathbf{u}_p) \otimes \mathbf{1}_{Q+1}$. Furthermore, notice that $\mathbf{H}_c$ does not depend on the subblock index p and contains all the *unknown* coefficients, whereas $\mathbf{W}_p$ contains all the *known* p-dependent complex exponentials which capture the channel's time variation in the BEM [c.f. (2)]. Following *Proposition 1*, we can rewrite (15) as

$$\tilde{\mathbf{y}}_p = (Q+1)^{-1} \mathbf{W}_p \mathbf{H}_c \left[\left(\mathbf{F}_M^{\mathcal{H}} \mathbf{u}_p \right) \otimes \mathbf{1}_{Q+1} \right] + \tilde{\mathbf{z}}_p. \quad (18)$$

Premultiplying $\tilde{\mathbf{y}}_p$ by $\mathbf{W}_p^{\mathcal{H}}$, we can annihilate the channel's variability, because $\mathbf{W}_p^{\mathcal{H}} \mathbf{W}_p = (Q+1)\mathbf{I}_{M(Q+1)}$, which also retains the noise whiteness.

Having removed time-variability (and thus, dependence on the subblock index p), we can now proceed with our second step of diagonalizing the I/O. Toward this objective, let us define $\tilde{\mathbf{F}}_M := [\mathbf{I}_{Q+1} \otimes \mathbf{f}_1, \ldots, \mathbf{I}_{Q+1} \otimes \mathbf{f}_M]$, where $\mathbf{f}_m$ is the mth column of the M-point FFT matrix $\mathbf{F}_M$. With $\mathbf{v}_p := \tilde{\mathbf{F}}_M \mathbf{W}_p^{\mathcal{H}} \tilde{\mathbf{y}}_p$, (18) yields

$$\mathbf{v}_p = \tilde{\mathbf{F}}_M \mathbf{H}_c \left[\left(\mathbf{F}_M^{\mathcal{H}} \mathbf{u}_p \right) \otimes \mathbf{1}_{Q+1} \right] + \mathbf{z}_p \quad (19)$$

where $\mathbf{z}_p$ remains white, since $\tilde{\mathbf{F}}_M$ is also unitary.

Because $\mathbf{H}_c$ in (17) has (column-) block-circulant structure, we show in Appendix B that it can be block-diagonalized using

$$\tilde{\mathbf{H}}_p := \begin{bmatrix} \tilde{\mathbf{H}}_{p,0}(0) & \mathbf{0}_{(Q+1)\times(Q+1)} & \ldots & \tilde{\mathbf{H}}_{p,0}(L) & \ldots & \tilde{\mathbf{H}}_{p,0}(1) \\ \tilde{\mathbf{H}}_{p,1}(1) & \tilde{\mathbf{H}}_{p,1}(0) & \ddots & \mathbf{0}_{(Q+1)\times(Q+1)} & \tilde{\mathbf{H}}_{p,1}(L) & \vdots \\ \vdots & \vdots & \ddots & & \ddots & \ddots \\ \tilde{\mathbf{H}}_{p,L}(L) & \tilde{\mathbf{H}}_{p,L}(L-1) & \ldots & \tilde{\mathbf{H}}_{p,L}(0) & \ldots & \mathbf{0}_{(Q+1)\times(Q+1)} \\ \vdots & \ddots & & & \ddots & \vdots \\ \mathbf{0}_{(Q+1)\times(Q+1)} & \ldots & \mathbf{0}_{(Q+1)\times(Q+1)} & \tilde{\mathbf{H}}_{p,M-1}(L) & \ldots & \tilde{\mathbf{H}}_{p,M-1}(0) \end{bmatrix} \quad (13)$$

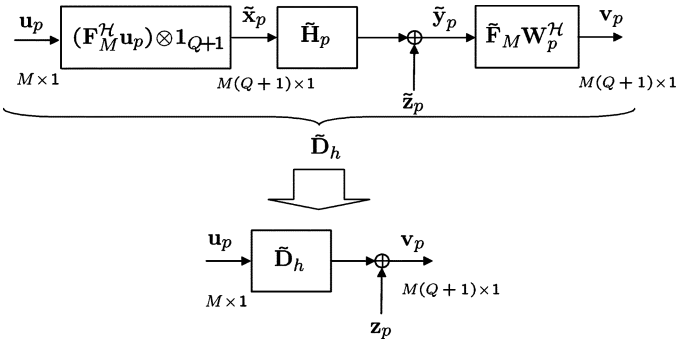

Fig. 4. System block diagram per subblock p of size $M(Q+1)$.

(I)FFT operations at the (transmitter) receiver. This fact allows one to rewrite (19) as (see also Fig. 4)

$$\mathbf{v}_p = \tilde{\mathbf{D}}_h\mathbf{u}_p + \mathbf{z}_p \tag{20}$$

where upon defining $\bar{\mathbf{h}}_q := [h_q(0),\ldots,h_q(L)]^T$, the (block) diagonal $\tilde{\mathbf{D}}_h$ is given by

$$\tilde{\mathbf{D}}_h = (Q+1)\left[\mathrm{diag}(\mathbf{V}_M\bar{\mathbf{h}}_0),\ldots,\mathrm{diag}(\mathbf{V}_M\bar{\mathbf{h}}_Q)\right]^T \tag{21}$$

with $\mathbf{V}_M$ denoting the matrix formed by the first $L+1$ columns of $\mathbf{F}_M$.

C. BD Recursion

According to (20), the BD-encoded block $\mathbf{u}_p$ that is encoded as $\tilde{\mathbf{x}}_p$ "sees" a block-diagonalized channel obtained in a process analogous to performing OFDM across $Q+1$ multipath channels, each with $L+1$ coefficients $\bar{\mathbf{h}}_q$. Inserting (4) into (20), we obtain

$$\mathbf{v}_p = \tilde{\mathbf{D}}_h\mathbf{D}_{g_p}\mathbf{u}_{p-1} + \mathbf{z}_p. \tag{22}$$

Matrix $\tilde{\mathbf{D}}_h$ has the two nice properties we were looking for: it is (block) diagonal; and it remains invariant across all P subblocks. The first property allows the interchange $\tilde{\mathbf{D}}_h\mathbf{D}_{g_p} = \mathbf{D}_{G_p}\tilde{\mathbf{D}}_h$, where $\mathbf{D}_{G_p} := \mathbf{I}_{Q+1}\otimes\mathbf{D}_{g_p}$, which leads to

$$\mathbf{v}_p = \mathbf{D}_{G_p}\tilde{\mathbf{D}}_h\mathbf{u}_{p-1} + \mathbf{z}_p. \tag{23}$$

The second property permits substitution of the *known* (previously received) subblock $\mathbf{v}_{p-1} = \tilde{\mathbf{D}}_h\mathbf{u}_{p-1} + \mathbf{z}_{p-1}$ into (23), through which we arrive at

$$\mathbf{v}_p = \mathbf{D}_{G_p}[\mathbf{v}_{p-1} - \mathbf{z}_{p-1}] + \mathbf{z}_p. \tag{24}$$

Equation (24) yields the I/O relationship we were seeking

$$\mathbf{v}_p = \mathbf{D}_{G_p}\mathbf{v}_{p-1} + \mathbf{z}'_p \tag{25}$$

where $\mathbf{z}'_p := \mathbf{z}_p - \mathbf{D}_{G_p}\mathbf{z}_{p-1}$ is AWGN with correlation matrix $2N_0\mathbf{I}_{M(Q+1)}$, since $\mathbf{D}_{G_p}$ is also unitary. This increase (by a factor of 2) in the noise variance confirms the SNR loss inherent to any differential detection [7].

IV. ML Detection

The ML-optimal detector for decoding $\mathbf{D}_{G_p}$ from $\mathbf{v}_p$ in (25) is given by

$$\hat{\mathbf{D}}_{G_p} = \arg\min_{\mathbf{D}_G\in\mathcal{A}_g^{M(Q+1)}} \|\mathbf{v}_p - \mathbf{D}_G\mathbf{v}_{p-1}\|^2 \tag{26}$$

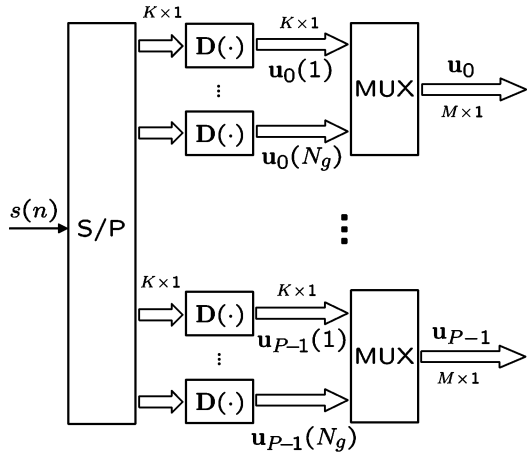

Fig. 5. BD encoder in (27).

where $\|\cdot\|$ denotes the Frobenius norm. Carrying out (26) incurs computational cost which increases exponentially with $M(Q+1)$. To reduce this complexity, we will adopt the grouping method of [12]. To this end, we further partition each $\mathbf{u}_p$ block of size M into N_g groups, each of size K. The overall transmitted subblock $\mathbf{u}_p(g)$ is (see also Fig. 5)

$$\mathbf{u}_p(g) = \begin{cases} \mathbf{D}_{g_p}(g)\mathbf{u}_{p-1}(g), & p\geq 1 \\ \mathbf{1}_{K\times 1}, & p=0 \end{cases} \tag{27}$$

with $\mathbf{u}_p(g)$ a $K\times 1$ vector, and $\mathbf{D}_{g_p}(g)$ a $K\times K$ matrix that maps the information symbols $\mathbf{s}_p(g)$. These subgroups can be indexed using N_g nonintersecting index subsets of size K, that we denote as $\{\mathcal{I}\}_{g=1}^{N_g}, \mathcal{I}_g = \{m_{g,1},\ldots,m_{g,K}\}$, and $[\mathbf{u}_p(g)]_k = [\mathbf{u}_p]_{m_{g,k}}$.

Following steps similar to those used to derive (20), the I/O relationship for the gth group of the pth subblock can now be written as $\mathbf{v}_p(g) = \tilde{\mathbf{D}}_h(g)\mathbf{u}_p(g) + \mathbf{z}(g)$, where $\tilde{\mathbf{D}}_h(g)$ is the grouped counterpart of $\tilde{\mathbf{D}}_h$ in (21), and is defined as

$$\tilde{\mathbf{D}}_h(g) := (Q+1)\left[\mathrm{diag}\left(\mathbf{V}_K(g)\bar{\mathbf{h}}_0\right),\ldots,\mathrm{diag}\left(\mathbf{V}_K(g)\bar{\mathbf{h}}_Q\right)\right]^T \tag{28}$$

where $\mathbf{V}_K(g)$ is a $K\times(L+1)$ Vandermonde matrix with (k,l)th entry $[\mathbf{V}_K(g)]_{k,l} = \exp[-j2\pi m_{g,k}(l-1)/M]$. We can now perform the differential recursion in (25) on a per-subgroup basis

$$\mathbf{v}_p(g) = \mathbf{D}_{G_p}(g)\mathbf{v}_{p-1}(g) + \mathbf{z}'(g) \tag{29}$$

and the reduced-complexity ML detector as

$$\hat{\mathbf{D}}_{G_p}(g) = \arg\min_{\mathbf{D}_G\in\mathcal{A}_g^{K(Q+1)}} \|\mathbf{v}_p(g) - \mathbf{D}_G\mathbf{v}_{p-1}(g)\|^2. \tag{30}$$

Without sacrificing ML optimality, we can further simplify (30), if we recall that our BD scheme entails N_g groups of size K carrying mutually independent symbols repeated $Q+1$ times [c.f. (4), (5), and (27)]. After dropping index g for brevity, we can rewrite (30) as

$$\begin{aligned}\hat{\mathbf{D}}_{g_p} &= \arg\min_{\mathbf{D}_g\in\mathcal{A}_g^{K(Q+1)}} \Big\{\|\mathbf{v}_p\|^2 + \|(\mathbf{I}_{Q+1}\otimes\mathbf{D}_g)\mathbf{v}_{p-1}\|^2 \\ &\qquad -2\mathrm{Re}\left\{\mathbf{v}_{p-1}^{\mathcal{H}}(\mathbf{I}_{Q+1}\otimes\mathbf{D}_g)^{\mathcal{H}}\mathbf{v}_p\right\}\Big\} \\ &= \arg\max_{\mathbf{D}_g\in\mathcal{A}_g^{K(Q+1)}} \sum_{k=0}^{K}\mathrm{Re}\left\{\left[\mathbf{D}_g^*\right]_{k,k}\sum_{q=0}^{Q} v_p^{(k,q)}v_{p-1}^{(k,q)*}\right\}\end{aligned} \tag{31}$$

where $v_p^{(k,q)} := [\mathbf{v}_p]_{k+qK}\ \forall k \in [1,K]$ and $q \in [1, Q+1]$.

V. Bandwidth Efficiency

In this section, we will specify P and M to optimize spectral efficiency. In our BD encoder (4), one subblock of size $M(Q+1)$ is used for initialization. The bandwidth efficiency, defined as the ratio of information-bearing symbols over the total number of transmitted symbols, is thus

$$\eta := \frac{(P-1)M(Q+1)}{N} \tag{32}$$

where $N = PM(Q+1) + PL(Q+1)$ and $PL(Q+1)$ is the number of redundant symbols, because we insert CP segments of length L every $P(Q+1)$ symbols. Since $M = N/(P(Q+1)) - L$, we can rewrite (32) as

$$\eta = 1 - \frac{L(Q+1)P}{N} - \frac{1}{P} + \frac{L(Q+1)}{N}. \tag{33}$$

For fixed parameters N, $\tau_{\max}$, $f_{\max}$, and T_s, corresponding to given channel parameters L and Q, we find that the maximum of η w.r.t. P occurs at

$$\frac{\partial \eta}{\partial P} = \frac{1}{P^2} - \frac{L(Q+1)}{N} = 0 \tag{34}$$

and the optimum P and M that maximize $(\partial^2\eta/\partial^2 P < 0)$ the efficiency are

$$P_{\text{opt}} = \left\lceil \sqrt{\frac{N}{L(Q+1)}} \right\rceil, \quad M_{\text{opt}} = \left\lceil \sqrt{\frac{NL}{Q+1}} - L \right\rceil. \tag{35}$$

Substituting (35) into (32), we obtain

$$\eta_{\text{opt}} = \left(1 - \sqrt{\frac{L(Q+1)}{N}}\right)^2. \tag{36}$$

Since $L \approx \tau_{\max}/T_s$ and $Q \approx 2f_{\max}T_sN$, we deduce that the maximum bandwidth efficiency and the optimum block size P achieving it are

$$\eta_{\text{opt}} \approx (1 - \sqrt{2f_{\max}\tau_{\max}})^2, \text{ and } P \approx \frac{1}{\sqrt{2f_{\max}\tau_{\max}}}. \tag{37}$$

Guaranteeing $2f_{\max}\tau_{\max} < 1$ in (37) explains why we confined application to underspread channels in *Assumption 1*.

Clearly, the efficiency decreases, together with L (or $\tau_{\max}$), because longer CP segments are inserted; and also with Q (or $f_{\max}$), because we fixed $N = P(M+L)(Q+1)$ in the optimization of η. If no multipath is present, then $L = 0$, and the efficiency loss is only due to the initial training block, which is negligible if we choose a sufficiently large P_{opt}. In any case, our system has the same efficiency as any BD-OFDM scheme with the same L, when the number of subcarriers is equal to M [12].

VI. Diversity and Coding-Gain Analyses

In this section, we will derive the diversity order and coding gain of our BD design in the high-SNR regime. The pairwise error probability (PEP) defines the probability that the ML detector incorrectly decodes an information block $\mathbf{D}_{G_p}(g)$ as $\mathbf{D}'_{G_p}(g)$. As usual, this PEP can be upper-bounded using the Chernoff bound [21]

$$\Pr\left[\mathbf{D}_G(g) \to \mathbf{D}'_G(g) | \mathbf{y}_{p-1}(g)\right] \le \exp\left[-\frac{d^2\left(\mathbf{D}_G(g), \mathbf{D}'_G(g)\right) E_s}{8N_0}\right] \tag{38}$$

with $d^2(\mathbf{D}_G(g), \mathbf{D}'_G(g)) := E_s^{-1}\|[\mathbf{D}_G(g) - \mathbf{D}'_G(g)]\mathbf{y}_{p-1}(g)\|^2$ and E_s denoting symbol energy. At high SNR, we can ignore the noise term in (29); so $\mathbf{y}_{p-1}(g) \approx \mathbf{D}_{G_p}(g)\tilde{\mathbf{D}}_h(g)\mathbf{u}_{p-1}(g)$, and the PEP becomes

$$\Pr\left[\mathbf{D}_G(g) \to \mathbf{D}'_G(g) | \mathbf{y}_{p-1}(g)\right] \le \exp\left[-\frac{\left\|[\mathbf{D}_G(g) - \mathbf{D}'_G(g)]\,\tilde{\mathbf{D}}_h(g)\mathbf{u}_{p-1}(g)\right\|^2}{8N_0}\right]. \tag{39}$$

Based on (28), we can rewrite $\tilde{\mathbf{D}}_h(g)\mathbf{u}_{p-1}(g) = \mathbf{D}_u(g)(\mathbf{I}_{Q+1} \otimes \mathbf{V}_K(g))\bar{\mathbf{h}}$, where $\mathbf{D}_u(g) := \text{diag}(\mathbf{u}_p(g))$ and $\bar{\mathbf{h}} := [\bar{\mathbf{h}}_0^T, \ldots, \bar{\mathbf{h}}_Q^T]^T$. Dropping indexes p and g for simplicity, the Euclidean distance $d^2(\mathbf{D}_G, \mathbf{D}'_G)$ becomes

$$\begin{aligned} &d^2\left(\mathbf{D}_G, \mathbf{D}'_G\right) \\ &\quad = E_s^{-1}\left\|[\mathbf{D}_G - \mathbf{D}'_G]\,\mathbf{D}_u(\mathbf{I}_{Q+1} \otimes \mathbf{V}_K)\bar{\mathbf{h}}\right\|^2 \\ &\quad = E_s^{-1}\bar{\mathbf{h}}^{\mathcal{H}}\left(\mathbf{I}_{Q+1} \otimes \mathbf{V}_K^{\mathcal{H}}\right)\mathbf{D}_u^{\mathcal{H}}\mathbf{D}_G^2\mathbf{D}_u(\mathbf{I}_{Q+1} \otimes \mathbf{V}_K)\bar{\mathbf{h}} \\ &\quad = \bar{\mathbf{h}}^{\mathcal{H}}\left(\mathbf{I}_{Q+1} \otimes \mathbf{V}_K^{\mathcal{H}}\right)\mathbf{D}_G^2(\mathbf{I}_{Q+1} \otimes \mathbf{V}_K)\bar{\mathbf{h}} \end{aligned} \tag{40}$$

where $\mathbf{D}_G^2 := [\mathbf{D}_G - \mathbf{D}'_G]^{\mathcal{H}}[\mathbf{D}_G - \mathbf{D}'_G]$, and we have used the fact that $\mathbf{D}_u^{\mathcal{H}}\mathbf{D}_u = E_s\mathbf{I}_{M(Q+1)}$ (notice that the entries of $\mathbf{u}$ have constant modulus).

The channel vector $\bar{\mathbf{h}}$ has correlation matrix $\mathbf{R}_h = E\{\bar{\mathbf{h}}\bar{\mathbf{h}}^{\mathcal{H}}\}$, with rank $r_h := \text{rank}(\mathbf{R}_h)$. If $\mathbf{R}_h$ is full rank, then $r_h = (Q+1)(L+1)$. Furthermore, we can decompose $\mathbf{R}_h = \mathbf{U}_h\mathbf{\Sigma}_h\mathbf{U}_h^{\mathcal{H}}$ where $\mathbf{\Sigma}_h := \text{diag}([\lambda_0, \ldots, \lambda_{r_h-1}])$ is an $r_h \times r_h$ diagonal matrix with the nonzero eigenvalues on the diagonal, and $\mathbf{U}_h$ is a $(Q+1)(L+1) \times r_h$ unitary matrix. Upon defining the $r_h \times 1$ prewhitened channel vector $\tilde{\mathbf{h}} := \mathbf{\Sigma}_h^{-1/2}\mathbf{U}_h^{\mathcal{H}}\bar{\mathbf{h}}$, we have $d^2(\mathbf{D}_G, \mathbf{D}'_G) = \tilde{\mathbf{h}}^{\mathcal{H}}\mathbf{A}_e\tilde{\mathbf{h}}$, where

$$\mathbf{A}_e := \mathbf{\Sigma}_h^{\frac{1}{2}}\mathbf{U}_h^{\mathcal{H}}\left(\mathbf{I}_{Q+1} \otimes \mathbf{V}_K^{\mathcal{H}}\right)\mathbf{D}_G^2(\mathbf{I}_{Q+1} \otimes \mathbf{V}_K)\mathbf{U}_h\mathbf{\Sigma}_h^{\frac{1}{2}}. \tag{41}$$

At high SNR, the average PEP can thus be expressed as

$$\Pr\left[\mathbf{D}_G \to \mathbf{D}'_G\right] \le \left(G_{e,c}\frac{E_s}{8N_0}\right)^{-G_{e,d}} \tag{42}$$

where $G_{e,d} := r_{A_e}$ and $G_{e,c} := \left(\prod_{r=0}^{r_{A_e}-1}\lambda_r\right)^{(1/r_{A_e})}$ are the diversity and coding gains, respectively. To achieve the maximum diversity gain $G_{d,\max}$, we need matrix $(\mathbf{I}_{Q+1} \otimes \mathbf{V}_K^{\mathcal{H}})\mathbf{D}_G^2(\mathbf{I}_{Q+1} \otimes \mathbf{V}_K)$ to have full rank. But notice that $(\mathbf{I}_{Q+1} \otimes \mathbf{V}_K^{\mathcal{H}})\mathbf{D}_G^2(\mathbf{I}_{Q+1} \otimes \mathbf{V}_K) = \mathbf{I}_{Q+1} \otimes (\mathbf{V}_K^{\mathcal{H}}\mathbf{D}_g^2\mathbf{V}_K)$. And because

$$\text{rank}\left[\mathbf{I}_{Q+1} \otimes \left(\mathbf{V}_K^{\mathcal{H}}\mathbf{D}_g^2\mathbf{V}_K\right)\right] = (Q+1)\text{rank}\left[\mathbf{V}_K^{\mathcal{H}}\mathbf{D}_g^2\mathbf{V}_K\right] \tag{43}$$

we need $\mathbf{V}_K^{\mathcal{H}}\mathbf{D}_g^2\mathbf{V}_K$ to have rank $(L+1)\ \forall \mathbf{D}_g \neq \mathbf{D}'_g$, which is achieved if $K \ge L+1$. So, with the $(Q+1)$ repetitions, IFFT/FFT, removal of the BEM's time variation at the receiver,

as well as the permutation matrices at both the transmitter/receiver sides, we have been able to achieve the maximum diversity of order $(Q+1)(L+1)$ provided by the doubly selective fading channel.

Now let us turn our attention to the coding gain. The coding gain G_c is defined as $G_c := \min_{\forall \mathbf{D}_g \neq \mathbf{D}'_g} G_{e,c}$, where $G_{e,c}$ is given by (42). If $\mathbf{R}_h$ has full rank, we obtain [c.f. (41)]

$$\begin{aligned} G_c &= \min_{\forall \mathbf{D}_g \neq \mathbf{D}'_g} [\det(\mathbf{A}_e)]^{\frac{1}{r_h}} \\ &= [\det(\mathbf{R}_h)]^{\frac{1}{r_h}} \\ &\quad \times \min_{\forall \mathbf{D}_g \neq \mathbf{D}'_g} \left[\det\left(\mathbf{I}_{Q+1} \otimes \left(\mathbf{V}_K^{\mathcal{H}} \mathbf{D}_g^2 \mathbf{V}_K\right)\right)\right]^{\frac{1}{r_h}}. \quad (44) \end{aligned}$$

Thus, we just need to find $\delta := \min_{\forall \mathbf{D}_g \neq \mathbf{D}'_g} \det(\mathbf{I}_{Q+1} \otimes (\mathbf{V}_K^{\mathcal{H}} \mathbf{D}_g^2 \mathbf{V}_K))$, which, based on the property $\det(\mathbf{A}_{M\times M} \otimes \mathbf{B}_{N\times N}) = (\det(\mathbf{A}))^N (\det(\mathbf{B}))^M$, can be written as $\delta = \min_{\forall \mathbf{D}_g \neq \mathbf{D}'_g} \det(\mathbf{V}_K^{\mathcal{H}} \mathbf{D}_g^2 \mathbf{V}_K)^{Q+1}$. Because we know that $\det(\mathbf{V}_K^{\mathcal{H}} \mathbf{D}_g^2 \mathbf{V}_K) = \det(\mathbf{V}_K^{\mathcal{H}} \mathbf{V}_K) \det(\mathbf{D}_g^2)$, maximizing this expression requires maximizing both $\det(\mathbf{V}_K^{\mathcal{H}} \mathbf{V}_K)$ and $\det(\mathbf{D}_g^2)$ at the same time. The former expression is maximized by choosing $\mathcal{I}_g = \{g, N_g + g, \ldots, LN_g + g\}$ (similar results can be found in [12]). The latter can be maximized after we use the fact that for a diagonal matrix $\mathbf{D}$, it holds that $\det(\mathbf{D}) = \prod_{i=1}^{N} d_{ii}$, with d_{ii} the ith diagonal element of $\mathbf{D}$. Then, $\det(\mathbf{D}_g^2) = \Delta_{\min,\mathcal{A}_g}$, where $\Delta_{\min,\mathcal{A}_g} := \prod_{i=1}^{K} |[\mathbf{D}_g]_{i,i} - [\mathbf{D}'_g]_{i,i}|^2$ is the product distance of vectors from the diagonal of $\mathbf{D}_g$ and $\mathbf{D}'_g$. Because $|\mathcal{A}_g| = |\mathcal{A}_s|^{Q+1}$, the product distance $\Delta_{\min,\mathcal{A}_g}$ decreases with $Q+1$, and so does the coding gain. Therefore, we deduce that the more pronounced time variability the channel provides, the higher order constellations we need to build, and thus, more SNR-shifted will be the BER curves.

VII. Numerical Results

To test our scheme, we generate TV channels using Jakes' model [9] with parameters $(f_c, T_s, f_{\max}, D)$, where D denotes the number of Doppler rays (here $D = 300$). The BEM approximates well Jakes' model in the least-squares (LS) sense when $Q/NT_s \geq f_{\max}$, and the LS fit has been validated in [14] and [11]. Since $\tau_{\max}$ and $f_{\max}$ are unknown, we work with their bounds and design our algorithm for the maximum allowed values of L and Q. Knowing these (L, Q) values, because $N = P(M+L)(Q+1)$, we take $K = M/(L+1)$ and select the subgroup size as $K(Q+1)$.

With rate $R = 1$, the alphabet of our BD encoder has size $|\mathcal{A}_g| = 2^{Q+1}$, and thus $\mathbf{D}_{g_p}(g)$ is chosen from a PSK constellation of size 2^{Q+1}. This testifies to the fact that our constellation size increases when time-selectivity is present $(Q \neq 0)$.

Four different channels will be considered depending on the time-frequency variability.

- Ch0: (Time-frequency flat) With $(L, Q) = (0, 0)$, the block-transmission parameters are chosen as $(N, P, M, K) = (1260, 1260, 1, 1)$. The bandwidth efficiency here is $\eta = (P-1)/P = 0.999$.
- Ch1: (Time-flat frequency-selective) To test the validity of our model in multipath, we generate a two-path channel $(L = 1)$ with coefficients $\bar{\mathbf{h}} := [h_0, h_1]^T$ chosen as zero-mean complex Gaussian with variances $\sigma_0^2 = \sigma_1^2 = 0.5$. With $(L, Q) = (1, 0)$, the chosen parameters are $(N, P, M, K) = (1260, 180, 6, 3)$, and result in efficiency $\eta = ((P-1)M)/(P(M+L)) = 0.852$.
- Ch2: (Time-selective frequency-flat) Here, we generate Jakes' model with $(f_c, T_s, f_{\max}, D) = (3.5\,\text{GHz}, 1\,\mu\text{s}, 810.2\,\text{Hz}, 300)$, corresponding to a maximum mobile velocity of $v = 250$ km/h. For $(L, Q) = (0, 2)$, maximum bandwidth efficiency suggests $M = 1$, and for this reason, we select $(N, P, M, K) = (1260, 420, 1, 1)$. The resultant efficiency is $\eta = (P-1)/P = 0.998$.
- Ch3: (doubly selective) Here, we simulate a channel with two $(L = 1)$ paths, each generated by Jakes' model using the same parameters as **Ch2** $(Q = 2)$. We generate the channel taps as in **Ch1**, and select $(N, P, M, K) = (1260, 60, 6, 3)$, which yields $\eta = ((P-1)M)/(P(M+L)) = 0.843$.

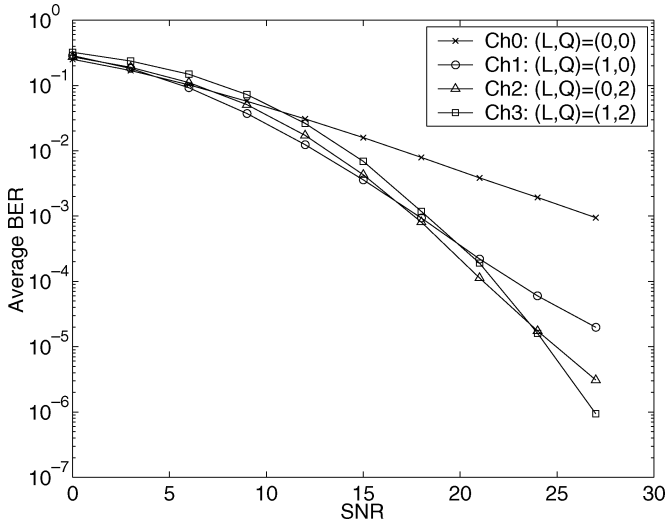

Fig. 6. Performance results for $(L, Q) = (0,0), (1,0), (0,2), (1,2)$.

In all simulations, SNR is defined as SNR $= E\{\|\mathbf{Hx}\|^2\}/E\{\|\mathbf{z}\|^2\}$.

1) Diversity Order: Using **Ch0–Ch3**, we will test our claims in Section VI about the diversity and coding gains provided by doubly selective channels, fully achieved by our differential design. By inspecting the slope of the bit-error rate (BER) curves in Fig. 6, we verify that the diversity order increases as L and/or Q increases. The repetition encoding employed when $Q > 0$ causes a parallel shift of the BER curves. Test case 3) will further quantify this shift. Note that for diversity orders above four, the BER improvement does not show up to SNRs of 25 dB or above, which suggests trading off diversity for reduced complexity by selecting small size blocks (over which $Q < 4$).

2) Comparison With [12]: In this simulation, we compare our differential modulation with the BD-OFDM scheme in [12]. This scheme enables maximum multipath diversity by dividing the OFDM subcarriers into subsets, giving rise to independent subchannels (this is related to our subgrouping scheme in Section IV). We will show that when dealing with time-invariant frequency-selective channels, our proposed design is, in fact, a

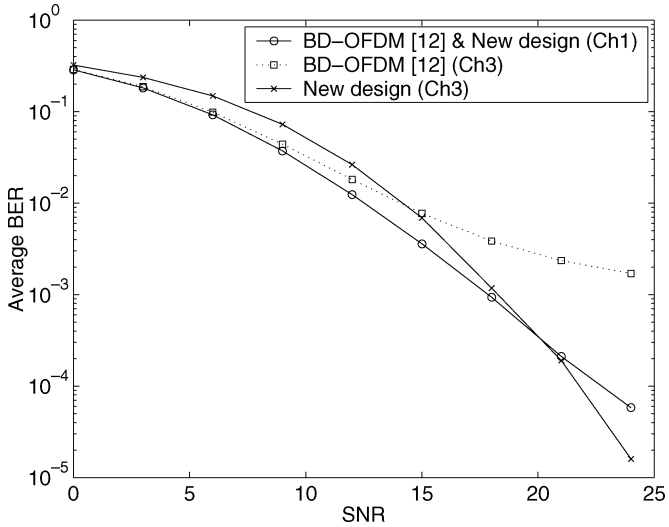

Fig. 7. Performance comparison with [12].

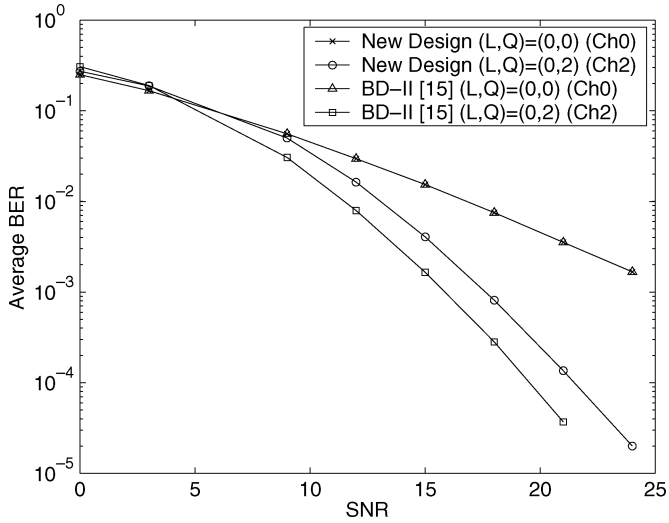

Fig. 8. Performance comparison with [15] over time-selective frequency-flat channels.

BD-OFDM scheme. Furthermore, if we allow arbitrary variation of the channel coefficients over time, BD-OFDM degrades; while our design not only shows resilience to time variations, but also takes full advantage of the Doppler and multipath diversity at the price of coding-gain loss. We will consider two cases.

Standard BD-OFDM over frequency-selective channels: Using **Ch1** with $(L,Q) = (1,0)$, $\mathbf{W}_p$ and $\mathbf{\Theta}$ are identity matrices; matrix $\tilde{\mathbf{F}}_M$ becomes $\mathbf{F}_M$; and matrix $\tilde{\mathbf{D}}_h(g)$ in (29) simplifies to $\tilde{\mathbf{D}}_h(g) = \mathrm{diag}(\mathbf{V}_K(g)\bar{\mathbf{h}})$, which coincides with the diagonal matrix employed by the BD-OFDM design of [12] for six subcarriers. Results are depicted in Fig. 7.

BD-OFDM over TV channels: Using the doubly selective **Ch3**, we compare also in Fig. 7 the performance of our design against the BD-OFDM design in [12] with the same number of subcarriers. Time-variability critically affects performance of OFDM-based transmissions. Our design, on the other hand, exploits the diversity provided by this doubly selective channel. The coding loss we experience, due to the repetition encoding, is clearly negligible, compared with the resilience we gain against time-variability.

3) Comparisons With [19] and [15]: Here, we compare our scheme with existing differential designs for two TV channels: first with a time-selective but frequency-flat channel, and second with a two-tap intersymbol interference (ISI)-inducing doubly selective channel. The latter will result in severe performance degradation of [15] and [19], which were designed for non-ISI environments. When implementing [19], we choose $N_B = 1,2,3$ and $N_B N_I = N$ for the rectangular interleaver, and $N^{DF} = 5$ feedback coefficients adaptively estimated using the recursive LS (RLS) algorithm, as in [19]. For the BD-II design in [15], we select the block size $P^{\mathrm{BD-II}}$ also equal to our parameter N.

Standard time-selective transmission: With the Jakes' model, as in **Ch2**, the average BER curves are shown in Fig. 8. Since both methods collect diversity at high SNR, the BER curves are parallel. For BER = 10^{-3} and $Q = 2$, our design is about 3 dB worse than [15], due to the loss in coding gain.

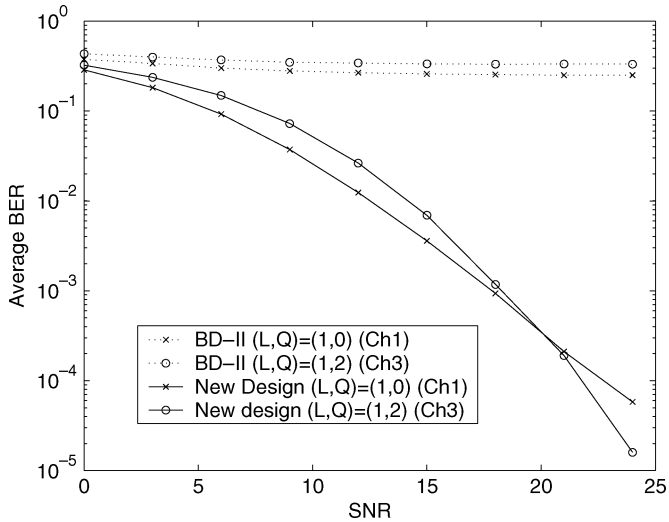

Fig. 9. Performance comparison with [15] over doubly selective channels.

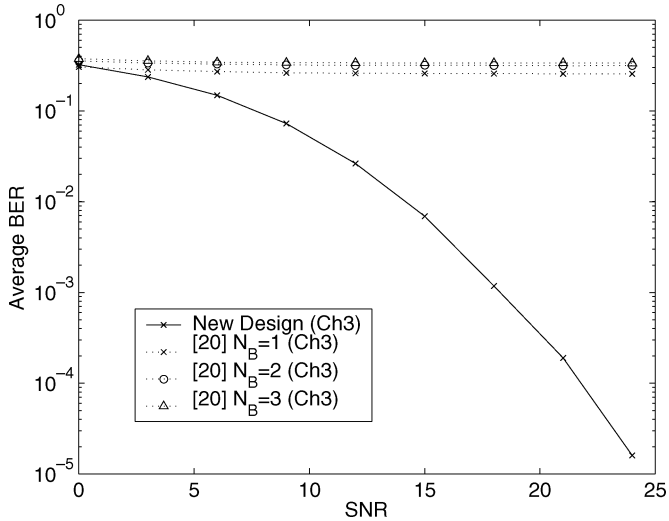

Fig. 10. Performance comparison with [19] over doubly selective channels.

Time-selective channel with ISI: With the doubly selective channel **Ch3**, Figs. 9 and 10 confirm that the performance of [19] and [15] severely degrades.

VIII. Concluding Remarks

We derived a BD scheme to by-pass estimation of general time- and frequency-selective channels. Our encoding (decoding) design includes four different stages at the transmitter (receiver): 1) Information (de)mapping and differential recursion; 2) (de)coding for channel diagonalization; 3) (de)interleaving for enabling diversity gains; and 4) CP insertion (removal) and P/S (S/P) transmission for block processing. We also derived a reduced-complexity ML detector in two stages: 1) using subgrouping; and 2) by taking advantage of the repeated information at the receiver to reduce complexity. Performance analysis and simulations confirmed that our BD design enables maximum multipath-Doppler diversity, with bandwidth efficiency (i.e., transmission rate) comparable to any BD-OFDM system at the expense of reduced coding gain, which is affordable for TV channels. Simulations have also corroborated that the novel design is particularly suitable for frequency-selective channels that undergo even slow ($Q < 4$) time variation per tap, and time-selective channels suffering from ISI. In both cases, our design outperforms differential OFDM derived for frequency-selective channels, and differential designs tailored for time-selective channels at medium-high SNR.

The next research steps will target doubly selective multiple-antenna links, as well as the much-needed (but so far unknown) capacity, or even achievable rates, to benchmark information rates over time-frequency wireless channels.

Appendix

A. Proof of Proposition 1

Consider the *fat* (row) block-diagonal $M(Q+1)\times M(Q+1)^2$ matrix

$$\tilde{\mathbf{W}}_p := \begin{bmatrix} \tilde{\mathbf{W}}_{p,0} & \mathbf{0} & \dots & \mathbf{0} \\ \mathbf{0} & \tilde{\mathbf{W}}_{p,1} & & \\ \vdots & & \ddots & \vdots \\ \mathbf{0} & \dots & \mathbf{0} & \tilde{\mathbf{W}}_{p,M-1} \end{bmatrix} \tag{45}$$

where using index $M_{p,q} := (p+q(Q+1))M + (p+q(Q+1)+1)L\ \forall p \in [0, P-1]$ and $q \in [0, Q]$, the $\tilde{\mathbf{W}}_p$ entries are $(Q+1)\times(Q+1)^2$ matrices $\tilde{\mathbf{W}}_{p,m}$ given by

$$\tilde{\mathbf{W}}_{p,m} := \begin{bmatrix} \mathbf{w}^T_{M_{p,0}+m} & \mathbf{0}^T_{Q+1} & \dots & \mathbf{0}^T_{Q+1} \\ \mathbf{0}^T_{Q+1} & \mathbf{w}^T_{M_{p,1}+m} & & \\ \vdots & & \ddots & \vdots \\ \mathbf{0}^T_{Q+1} & \dots & \mathbf{0}^T_{Q+1} & \mathbf{w}^T_{M_{p,Q}+m} \end{bmatrix}. \tag{46}$$

Define also the *tall* (column) block-circulant $M(Q+1)^2 \times M(Q+1)$ matrix

$$\tilde{\mathbf{H}}_c := \begin{bmatrix} \tilde{\mathbf{H}}_c(0) & \mathbf{0} & \dots & \tilde{\mathbf{H}}_c(L) & \dots & \tilde{\mathbf{H}}_c(1) \\ \tilde{\mathbf{H}}_c(1) & \tilde{\mathbf{H}}_c(0) & \ddots & \mathbf{0} & \tilde{\mathbf{H}}_c(L) & \vdots \\ \vdots & \vdots & \ddots & & \ddots & \ddots \\ \tilde{\mathbf{H}}_c(L) & \tilde{\mathbf{H}}_c(L-1) & \dots & \tilde{\mathbf{H}}_c(0) & \dots & \mathbf{0} \\ \vdots & \ddots & & & \ddots & \vdots \\ \mathbf{0} & \dots & \mathbf{0} & \tilde{\mathbf{H}}_c(L) & \dots & \tilde{\mathbf{H}}_c(0) \end{bmatrix} \tag{47}$$

where $\tilde{\mathbf{H}}_c(l)$ is a $(Q+1)^2\times(Q+1)$ matrix with $\mathbf{h}(l)$ repeated $(Q+1)$ times; i.e., $\tilde{\mathbf{H}}_c(l) := \mathbf{I}_{Q+1}\otimes\mathbf{h}(l)$.

Recalling (2) and using (45) and (47), we can separate the complex exponentials from the time-invariant coefficients and express the channel matrix $\tilde{\mathbf{H}}_p$ as

$$\tilde{\mathbf{H}}_p = \tilde{\mathbf{W}}_p\tilde{\mathbf{H}}_c. \tag{48}$$

Notice that if the channel is time-invariant ($Q=0$), then $\tilde{\mathbf{W}}_p$ is an $M\times M$ identity matrix, and $\tilde{\mathbf{H}}_c$ is a standard circulant matrix that can be diagonalized and differentially encoded using OFDM [12]. On the other hand, if the channel is frequency-flat ($L=0$), $\tilde{\mathbf{H}}_p$ is diagonal, and BD encoding can be performed as in [15].

We will show that when the input $\tilde{\mathbf{x}}_p$ has the repetitive structure $\tilde{\mathbf{x}}_p = (\mathbf{F}^{\mathcal{H}}_M\mathbf{u}_p)\otimes\mathbf{1}_{Q+1}$, the channel matrix $\tilde{\mathbf{H}}_p$ can afford a factorization similar to (48), but with both factors, call them now $\mathbf{W}_p$ and $\mathbf{H}_c$, being square matrices (as opposed to (48), where $\tilde{\mathbf{W}}_p$ is *fat* and $\tilde{\mathbf{H}}_c$ is *tall*). Toward this objective, we can easily verify by direct substitution the following lemmas.

Lemma 1: If $\tilde{\boldsymbol{\alpha}} := \alpha\otimes\mathbf{1}_{Q+1}$, then $\tilde{\mathbf{H}}_c(l)\tilde{\boldsymbol{\alpha}} = (Q+1)^{-1}(\mathbf{1}_{Q+1}\otimes\mathbf{H}_c(l))\tilde{\boldsymbol{\alpha}}$, where $\mathbf{H}_c(l) := \mathbf{1}^T_{Q+1}\otimes\mathbf{h}(l)$.

Lemma 2: If $\tilde{\boldsymbol{\Pi}} := \mathbf{1}_{Q+1}\otimes\boldsymbol{\Pi}$, then $\tilde{\mathbf{W}}_{p,m}\tilde{\boldsymbol{\Pi}} = (\mathbf{1}^T_{Q+1}\otimes\mathbf{W}_{p,m})\boldsymbol{\Pi}$, where $\mathbf{W}_{p,m} := [\mathbf{w}_{M_{p,0}+m},\dots,\mathbf{w}_{M_{p,Q}+m}]^T$.

Because of the repeated structure of $\tilde{\mathbf{x}}_p$, *Lemmas 1* and *2* imply that $\mathbf{1}_{Q+1}\otimes\mathbf{H}_c(l) = (\mathbf{1}_{Q+1}\otimes\mathbf{I}_{Q+1})\mathbf{H}_c(l)$ and $\mathbf{1}^T_{Q+1}\otimes\mathbf{W}_{p,m} = \mathbf{W}_{p,m}(\mathbf{1}^T_{Q+1}\otimes\mathbf{I}_{Q+1})$. Furthermore, using the identity $(\mathbf{1}^T_{Q+1}\otimes\mathbf{I}_{Q+1})(\mathbf{1}_{Q+1}\otimes\mathbf{I}_{Q+1}) = (Q+1)^{-1}\mathbf{I}_{Q+1}$, we obtain

$$\tilde{\mathbf{W}}_{p,m}\tilde{\mathbf{H}}_c(l) = (Q+1)^{-1}\mathbf{W}_{p,m}\mathbf{H}_c(l). \tag{49}$$

Based on (49), we can restructure the submatrices $\tilde{\mathbf{W}}_{p,m}$ and $\tilde{\mathbf{H}}_c(l)$ in (45) and (47) into two $(Q+1)\times(Q+1)$ square submatrices, and thus obtain two $M(Q+1)\times M(Q+1)$ square factors $\mathbf{W}_p$ and $\mathbf{H}_c$, allowing us to write (48) as

$$\tilde{\mathbf{W}}_p\tilde{\mathbf{H}}_c = (Q+1)^{-1}\mathbf{W}_p\mathbf{H}_c. \tag{50}$$

Substituting the latter into (15) completes the proof of *Proposition 1*.

B. Derivation of (20)

We can readily simplify the right-hand side of (19) as

$$\mathbf{H}_c\left[(\mathbf{F}^{\mathcal{H}}_M\mathbf{u}_p)\otimes\mathbf{1}_{Q+1}\right] = (Q+1)^{-1}\bar{\mathbf{H}}_c\mathbf{F}^{\mathcal{H}}_M\mathbf{u}_p \tag{51}$$

where the $M(Q+1)\times M$ matrix $\bar{\mathbf{H}}_c$ is (column-wise) vector-circulant with the first column generated as $[\mathbf{h}^T(0),\dots,\mathbf{h}^T(L),\mathbf{0}^T_{Q+1},\dots,\mathbf{0}^T_{Q+1}]^T$. Such a matrix can be converted into a set of $Q+1$ circulant $M\times M$ matrices $\mathbf{C}_q$ (with the first column $[h_q(0),\dots,h_q(L),0,\dots,0]^T$) after multiplying by a proper permutation matrix $\boldsymbol{\Gamma}$ to obtain

$$\tilde{\mathbf{F}}_M\bar{\mathbf{H}}_c\mathbf{F}^{\mathcal{H}}_M = \tilde{\mathbf{F}}_M\boldsymbol{\Gamma}\begin{bmatrix}\mathbf{C}_0\\ \vdots \\ \mathbf{C}_Q\end{bmatrix}\mathbf{F}^{\mathcal{H}}_M \tag{52}$$

where $\mathbf{\Gamma} := [\mathbf{I}_{Q+1} \otimes \mathbf{e}_1, \ldots, \mathbf{I}_{Q+1} \otimes \mathbf{e}_M]^T$, with $\mathbf{e}_m$ being the mth row of $\mathbf{I}_M$. Since $\tilde{\mathbf{F}}_M \mathbf{\Gamma} = \mathbf{I}_{Q+1} \otimes \mathbf{F}_M$, we arrive at

$$(\mathbf{I}_{Q+1} \otimes \mathbf{F}_M) \begin{bmatrix} \mathbf{C}_0 \\ \vdots \\ \mathbf{C}_Q \end{bmatrix} \mathbf{F}_M^{\mathcal{H}} = \begin{bmatrix} \mathbf{F}_M \mathbf{C}_0 \mathbf{F}_M^{\mathcal{H}} \\ \vdots \\ \mathbf{F}_M \mathbf{C}_Q \mathbf{F}_M^{\mathcal{H}} \end{bmatrix}. \quad (53)$$

Each $M \times M$ matrix $\mathbf{C}_q$ in (53) is circulant and can be diagonalized after applying the well-known property of circulant matrices [5, p. 202]: $\mathbf{C}_q = \mathbf{F}_M^{\mathcal{H}} \mathrm{diag}(\mathbf{V}_M \bar{\mathbf{h}}_q) \mathbf{F}_M$, where $\mathbf{V}_M$ is an $M \times (L+1)$ matrix containing the first $L+1$ columns of $\mathbf{F}_M$ and $\bar{\mathbf{h}}_q := [h_q(0), \ldots, h_q(L)]^T$. Substituting $\mathbf{C}_q$ into (53), we obtain

$$\tilde{\mathbf{D}}_h := \left[\mathrm{diag}(\mathbf{V}_M \bar{\mathbf{h}}_0), \ldots, \mathrm{diag}(\mathbf{V}_M \bar{\mathbf{h}}_Q)\right]^T. \quad (54)$$

ACKNOWLEDGMENT

A. Cano would like to thank G. B. Giannakis for the opportunity to visit SPinCOM at the University of Minnesota during Spring–Fall 2004, where this work was performed.

REFERENCES

[1] K. L. Baum and N. S. Nadgauda, "A comparison of differential and coherent reception for a coded OFDM system in a low C/I environment," in *Proc. GLOBECOM Conf.*, Phoenix, AZ, 1997, pp. 300–304.

[2] S. Bhashyam, A. M. Sayeed, and B. Aazhang, "Time-selective signaling and reception for communication over multipath fading channels," *IEEE Trans. Commun.*, vol. 48, no. 1, pp. 83–94, Jan. 2000.

[3] Y. E. Dallal and S. Shamai, "Time diversity in DPSK noisy phase channels," *IEEE Trans. Commun.*, vol. 40, no. 11, pp. 1703–1715, Nov. 1992.

[4] G. B. Giannakis and C. Tepedelenlioglu, "Basis expansion models and diversity techniques for blind identification and equalization of time-varying channels," *Proc. IEEE*, vol. 86, no. 11, pp. 1969–1986, Nov. 1998.

[5] G. H. Golub and C. Loan, *Matrix Computations*, 3 ed. Baltimore, MD: Johns Hopkins Univ. Press, 1996.

[6] P. Ho and D. Fung, "Error performance of multiple-symbol differential detection of PSK signals transmitted over correlated Rayleigh fading channels," *IEEE Trans. Commun.*, vol. 40, no. 10, pp. 1566–1569, Oct. 1992.

[7] B. M. Hochwald and W. Sweldens, "Differential unitary space–time modulation," *IEEE Trans. Commun.*, vol. 48, no. 12, pp. 2041–2052, Dec. 2000.

[8] B. L. Hughes, "Differential space–time modulation," *IEEE Trans. Inf. Theory*, vol. 46, no. 11, pp. 2567–2578, Nov. 2000.

[9] W. C. Jakes, *Microwave Mobile Communications*. New York: Wiley, 1974.

[10] Y. Larsen, G. Leus, and G. B. Giannakis, "Constant modulus and reduced PAPR block differential encoding for frequency-selective channels," *IEEE Trans. Commun.*, vol. 52, no. 4, pp. 622–631, Apr. 2004.

[11] G. Leus, S. Zhou, and G. B. Giannakis, "Orthogonal multiple access over time- and frequency-selective channels," *IEEE Trans. Inf. Theory*, vol. 49, no. 8, pp. 1942–1950, Aug. 2003.

[12] Z. Liu and G. B. Giannakis, "Block differentially encoded OFDM with maximum multipath diversity," *IEEE Trans. Wireless Commun.*, vol. 2, no. 3, pp. 420–423, May 2003.

[13] Z. Liu, Y. Xin, and G. B. Giannakis, "Linear constellation precoding for OFDM with maximum multipath diversity and coding gains," *IEEE Trans. Commun.*, vol. 51, no. 3, pp. 416–427, Mar. 2003.

[14] X. Ma and G. B. Giannakis, "Maximum-diversity transmissions over doubly selective wireless channels," *IEEE Trans. Inf. Theory*, vol. 49, no. 7, pp. 1832–1840, Jul. 2003.

[15] X. Ma, G. B. Giannakis, and B. Lu, "Block differential encoding for rapidly fading channels," *IEEE Trans. Commun.*, vol. 52, no. 3, pp. 416–425, Mar. 2004.

[16] X. Ma, G. B. Giannakis, and S. Ohno, "Optimal training for block transmissions over doubly selective wireless fading channels," *IEEE Trans. Signal Process.*, vol. 51, no. 5, pp. 1351–1366, May 2003.

[17] J. G. Proakis, *Digital Communications*, 4 ed. New York: McGraw-Hill, 2001.

[18] A. M. Sayeed and B. Aazhang, "Joint multipath-Doppler diversity in mobile wireless communications," *IEEE Trans. Commun.*, vol. 47, no. 1, pp. 123–132, Jan. 1999.

[19] R. Schober and L. H. J. Lampe, "Differential modulation diversity," *IEEE Trans. Veh. Technol.*, vol. 51, no. 6, pp. 1431–1444, Nov. 2002.

[20] ——, "Noncoherent receivers for differential space–time modulation," *IEEE Trans. Commun.*, vol. 50, no. 5, pp. 768–777, May 2002.

[21] V. Tarokh, N. Seshadri, and A. R. Calderbank, "Space–time codes for high data rate wireless communication: Performance criterion and code construction," *IEEE Trans. Inf. Theory*, vol. 44, no. 3, pp. 744–765, Mar. 1998.

Alfonso Cano (S'01) received the B.Sc. and M.Sc. degrees in electrical engineering from the Universidad Carlos III de Madrid, Madrid, Spain, in 2002. Since then, he has been working toward the Ph.D. degree, first with the Department of Signal Theory and Communications, Universidad Carlos III de Madrid, and since 2003, in the area of Signal Theory and Communications, Universidad Rey Juan Carlos, Madrid, Spain.

His research interests lie in the areas of signal processing and communications, including space–time coding, time-frequency selective channels, multicarrier, and cooperative communication systems.

Xiaoli Ma (M'03) received the B.S. degree in automatic control from Tsinghua University, Beijing, P.R. China, in 1998, and the M.Sc. and Ph.D. degrees in electrical engineering from the University of Virginia, Charlottesville, in 1999, and the University of Minnesota, Minneapolis, in 2003, respectively.

Since August 2003, she has been an Assistant Professor with the Department of Electrical and Computer Engineering, Auburn University, Auburn, AL. Her research interests include transceiver design for wireless fading channels, communications over time- and frequency-selective channels, complex-field coding, channel estimation and equalization algorithms, and carrier-frequency synchronization for OFDM systems.

Georgios B. Giannakis (F'97) received the Diploma in electrical engineering from the National Technical University of Athens, Athens, Greece, in 1981, and the M.Sc. degrees in electrical engineering in 1983 and mathematics in 1986, and the Ph.D. degree in electrical engineering in 1986 from the University of Southern California (USC), Los Angeles, CA.

After lecturing for one year at USC, he joined the University of Virginia in 1987, where he became a Professor of Electrical Engineering in 1997. Since 1999 he has been a Professor with the Department of Electrical and Computer Engineering, University of Minnesota, Minneapolis, where he now holds an ADC Chair in Wireless Telecommunications. His general interests span the areas of communications and signal processing, estimation and detection theory, time-series analysis, and system identification—subjects on which he has published more than 220 journal papers, 380 conference papers, and two edited books. Current research focuses on transmitter and receiver diversity techniques for single- and multiuser fading communication channels, complex-field and space–time coding, multicarrier, ultra-wideband wireless communication systems, cross-layer designs, and sensor networks.

Dr. Giannakis is the (co-) recipient of six paper awards from the IEEE Signal Processing (SP) and Communications Societies (1992, 1998, 2000, 2001, 2003, 2004). He received Technical Achievement Awards from the SP Society in 2000 and EURASIP in 2005. He served as Editor-in-Chief for the IEEE SIGNAL PROCESSING LETTERS, as Associate Editor for the IEEE TRANSACTIONS ON SIGNAL PROCESSING, and the IEEE SIGNAL PROCESSING LETTERS, as Secretary of the SP Conference Board, as Member of the SP Publications Board, as Member and Vice-Chair of the Statistical Signal and Array Processing Technical Committee, as Chair of the SP for Communications Technical Committee, and as a Member of the IEEE Fellows Election Committee. He has also served as a Member of the IEEE-SP Society's Board of Governors, the Editorial Board for the PROCEEDINGS OF THE IEEE, and the Steering Committee of the IEEE TRANSACTIONS ON WIRELESS COMMUNICATIONS.